Simple and Effective Online Position Error Compensation Method for Sensorless SPMSM Drives

Wang, Hechao; Lu, Kaiyuan; Wang, Dong; Blaabjerg, Frede

Published in:
IEEE Transactions on Industry Applications

DOI (link to publication from Publisher):
10.1109/TIA.2019.2958792

Publication date:
2020

Document Version
Accepted author manuscript, peer reviewed version

This article has been accepted for publication in a future issue of this journal, but has not been fully edited. Content may change prior to final publication. Citation information: DOI 10.1109/TIA.2019.2958792, IEEE Transactions on Industry Applications

Simple and Effective Online Position Error Compensation Method for Sensorless SPMSM Drives

Hechao Wang
Department of. energy technology
Aalborg University
Aalborg Denmark
hec@et.aau.dk

Kaiyuan Lu
Department of. energy technology
Aalborg University
Aalborg Denmark
klu@et.aau.dk

Dong Wang
Department of. energy technology
Aalborg University
Aalborg Denmark
dwa@et.aau.dk

Frede Blaabjerg
Department of. energy technology
Aalborg University
Aalborg Denmark
fbl@et.aau.dk

***Abstract*—In low-speed sensorless control of Surface Mounted Permanent Magnet Synchronous Machine (SPMSM), High Frequency (HF) signal injection methods are often used to estimate the rotor position by tracking the motor saliency characterized by the inductances. Cross-saturation effects caused by the load current will influence the inductances and consequently the saliency, which will introduce position estimation error to the sensorless drive, degrading the drive performance. Such load-dependent position estimation error, which is inherent in HF signal injection sensorless methods, is difficult to be identified by the sensorless algorithm itself. This paper proposes a new online method to detect and compensate the load-dependent position estimation error for SPMSM without additional devices or the knowledge of the load-dependent HF inductances. The proposed method can identify effectively the load-dependent position estimation error by simply varying the direction of the current vector. Experimental results are presented to validate the proposed solution.**

***Keywords*—SPMSM, sensorless, position estimation error compensation.**

I. INTRODUCTION

In Surface Mounted Permanent Magnet Synchronous Machine (SPMSM) drive systems, it is preferred to employ sensorless methods to reduce the cost and increase the reliability [1]. Sensorless methods are often categorized by the operating speed, i.e. medium-high speed and low speed, respectively [2-7]. In the medium-high speed range, the fundamental frequency machine voltage equation is often used to obtain the rotor position information contained in the machine back-EMF voltage [2]. In the low speed range, due to the low back-EMF voltage, High Frequency (HF) signal injection methods based on the HF machine voltage equation are used to detect the rotor position by tracking the motor inductance saliency. Typical methods are sinusoidal signal injection in the αβ-reference frame [3] or in the estimated dq-reference frame [4]; square-wave signal injection [5] and pulse-based injection methods [6, 7], etc.

The direction of the rotor d-axis is aligned with the rotor north pole of PMSM. Often the d-axis is slight saturated by the permanent magnet flux, which introduces a small saliency to the SPMSM. However the cross-saturation effects caused by the load current will influence the motor inductances and consequently the orientation of the motor saliency [17]. Independent of the injection scheme chosen, this phenomenon will influence the accuracy of the position estimation for HF injection based sensorless drive [17]. This load-dependent position estimation error is an inherent feature in HF injection sensorless methods, which is difficult to be corrected by the sensorless methods themselves [18].

Using Finite Element Analysis could accurately calculate machine HF self- and mutual- inductances at different loads for determining this load-dependent position error. But this requires detailed knowledge of the machine which is often not available for the end users [9]. These HF inductances or detailed machine flux-map may also be obtained through dedicated offline measurements [10]. The main challenge here is that since this error is load-dependent, during the measurement, the machine has to be locked while the load current is present for keeping the machine at standstill. Extra shaft locking device is therefore needed and this is not convenient. To solve this problem, attempts have been made to maintain a quasi-standstill condition with special injection signals for obtaining the machine flux-map without rotor locking [23-26]. However, accurate terminal voltage information is always needed, which requires dedicate hardware for PWM voltage measurement or accurate inverter voltage error compensation.

An alternative solution could be to utilize the estimated position from the back-EMF sensorless method as a reference since the cross-saturation effects have limited influence on the back-EMF based sensorless methods [13]. Therefore, in medium-high speed range, with back-EMF sensorless method applied, the HF inductances could be obtained by injecting HF signal [14]. This requires implementing back-EMF and HF injection sensorless methods together in the medium-high speed operation range, where the position estimated from back-EMF based sensorless methods is taken as the reference (real) position [13]. However, in contrast to the statement in [13], the cross-saturation effects caused significant position estimation error in the extended back-EMF based sensorless method [27]. This complicates the situation if the back-EMF based sensorless method can provide a reliable reference position for correcting the position estimated from the HF injection based sensorless method or not.

This article has been accepted for publication in a future issue of this journal, but has not been fully edited. Content may change prior to final publication. Citation information: DOI 10.1109/TIA.2019.2958792, IEEE Transactions on Industry Applications

These methods either need detailed knowledge of the machine geometry, or accurate voltage measurement together with (preferably) an additional shaft-locking device, introducing application inconveniences. Attempt has been made to acquire this load dependent position error without a shaft locking device and voltage measurement. This turns out to be not easy, since the measurement has to be performed with the q-axis current present and driving torque will be generated. Injection of pulsed q-axis currents (torques) with opposite directions to the machine to keep it at nearly standstill has been tried in [11]. Then during this short duration with saturation introduced by the q-axis current, the resultant position estimation error may be obtained by parabolic curve fitting with the assumptions of a small position estimation error, constant dq-axes inductances, neglected resistive voltage drop, etc. [11]. However, it may be noticed that almost all the existing position estimation methods are based on the machine voltage equation, which by nature is affected by the cross-saturation effects. As a matter of fact, the cross-coupling effects have limited influences in the torque equation for SPMSM. In this paper, a new attempt to utilize the torque equation to online identify this load-dependent position error is fully explored. The method turns out to be simple to use and it gives satisfactory results.

In this paper, the analysis of the cross-saturation effects on the sensorless drive, as briefly discussed in the previous conference paper [19], is elaborated. The load-dependent position estimation error detection method using the torque equation is fully examined. Moreover, a new online detection method is proposed in this paper to help reduce the calculation burden compared with the method proposed in the previous conference paper [19] for SPMSM. Based on the proposed method, the real online position estimation error identification/compensation method could be achieved without affecting the pulse-based injection sensorless control method for normal sensorless operation of the drive. The motor load-dependent HF inductance information or additional devices (a rotor-locker or a special load system) are not required. The proposed method could online detect and compensate the load-dependent position estimation error simply and effectively, which has been verified experimentally.

This paper is organized in the following manner. In section II, the machine HF model used for position estimation in the low speed range is presented with the influence of the cross-saturation effects as well as the load-dependent position estimation error explained. In section III, the proposed on-line identification/compensation methods based on the PMSM torque equation, with or without the reluctance torque component, are explained in detail. The experimental verifications of the proposed online detection method are given in section IV. Section V concludes this paper.

II. Fundamentals of PMSM Sensorless Control with Load-dependent Position Estimation Error

A sensorless Field Oriented Control (FOC) system of PMSM is shown in Fig. 1. In the low speed range, HF signal injection method is employed to obtain the rotor position, which is essential for reference frame transformations in the FOC system. In this paper, to avoid the uncertainties of motor terminal voltages and motor parameters, only measured line currents are used in the position estimation. Meanwhile, in order to avoid the filters used in the sensorless algorithm, pulsed signal injection method similar to [7], which will be illustrated in the following part, is used in this paper. In the SPMSM drive system, the angle β between the current vector and the d-axis is often set to 90 electrical degrees, and the d-axis current command is zero. In order to keep the electromagnetic torque constant with different current vector angle β, the drive system is operated in speed control mode as illustrated in Fig. 1. Speed control can find many industrial applications such as pumps and fans.

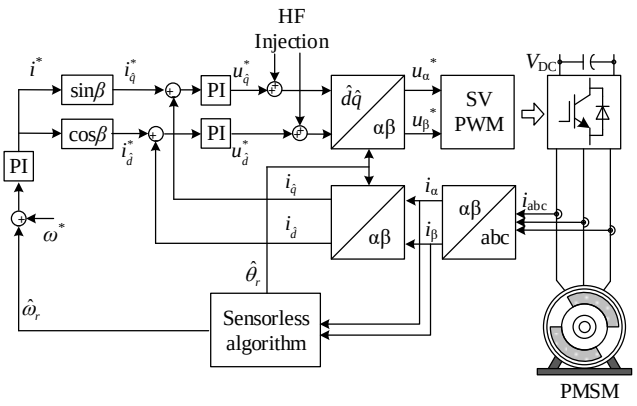

Fig. 1. Tranditional sensorless drive system.

The voltage equations of the PMSM in the machine real dq-reference frame are shown as:

$$\begin{bmatrix} u_d \\ u_q \end{bmatrix} = R\begin{bmatrix} i_d \\ i_q \end{bmatrix} + \frac{d}{dt}\begin{bmatrix} \lambda_d \\ \lambda_q \end{bmatrix} + \omega_r \begin{bmatrix} 0 & -1 \\ 1 & 0 \end{bmatrix}\begin{bmatrix} \lambda_d \\ \lambda_q \end{bmatrix}$$
$$\begin{bmatrix} \lambda_d \\ \lambda_q \end{bmatrix} = \begin{bmatrix} L_d & L_{dq} \\ L_{qd} & L_q \end{bmatrix}\begin{bmatrix} i_d \\ i_q \end{bmatrix} + \lambda_{mpm}\begin{bmatrix} 1 \\ 0 \end{bmatrix} \quad (1)$$

where u_d, u_q, i_d, i_q are the stator dq-axes voltages and currents respectively; L_d, L_q are the dq-axes self-inductances respectively; $L_{dq} = L_{qd}$ [16] are the cross-coupling inductances caused by the cross-saturation effects due to the load current; R is the stator resistance; ω_r is the rotor electrical speed; λ_d, λ_q are the dq-axes flux linkages respectively and λ_{mpm} is the peak value of the rotor PM flux linkage.

To estimate the rotor position, two pulsed voltage vectors ($\vec{U}_{\hat{d}}$) with opposite directions are injected in two switching periods successively as shown in Fig. 2(a), where $i_{\hat{q}\_[k-2]}$ is the sampled current at the beginning of the [k-2]th switching period; $\Delta(\Delta i_{\hat{q}})_{\_[k]}$ is calculated in the [k]th switching period based on

This article has been accepted for publication in a future issue of this journal, but has not been fully edited. Content may change prior to final publication. Citation information: DOI 10.1109/TIA.2019.2958792, IEEE Transactions on Industry Applications

the previous three sampled currents $i_{\hat{q}\_[k-2]}$, $i_{\hat{q}\_[k-1]}$ and $i_{\hat{q}\_[k]}$. The voltage command for FOC is held constant for these two switching periods during the opposite pulsed voltage vector injections (Fig. 2(a)). This is to avoid additional current variation that may be introduced by different FOC voltage commands in these two switching periods. The controller is therefore updated at half of the switching frequency.

This method is similar to the square wave pulsating injection method [5]. The signal processing part has been modified to avoid using filters and it is a simple (no filters) and effective method [28]. This method is therefore adopted in this paper for normal sensorless operation of the drive. For PMSM drive, to reduce the current ripple on the q-axis (thus the torque), it is preferred to inject voltage vectors on the estimated d-axis ($\hat{d}$). The obtained current variation $\Delta(\Delta i_{\hat{q}})$, fed to a Phase-Locked Loop (PLL) to generate the estimated position (Fig. 2(b)), is updated every two switching periods as well.

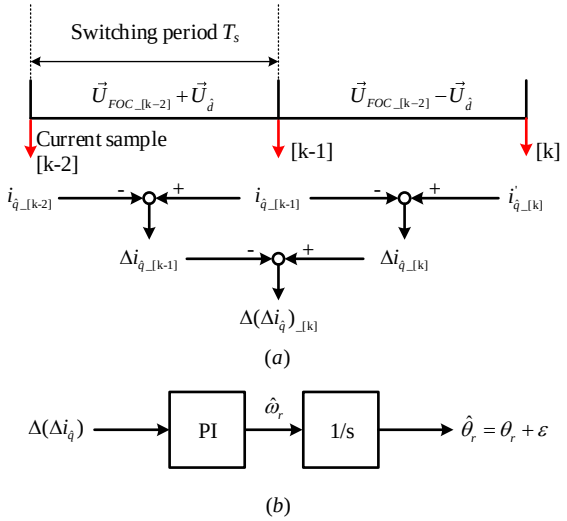

Fig. 2. Implementation of the pulsed injection method for sensorless control. (a) Injection scheme, (b) PLL for position estimation.

When considering machine small signals at a much higher frequency than the fundamental frequency, it may be assumed that the resistive voltage drop, and back-EMF voltage component, etc., do not change during two neighboring switching periods [7]. Therefore, based on the aforementioned pulse injection scheme, by applying (1) in the first and second switching periods respectively and then subtracting these two voltage equations, (1) is reduced to [7]:

$$\begin{bmatrix}\Delta u_d\\ \Delta u_q\end{bmatrix}\approx\begin{bmatrix}L_{d\_HF}(i_d,i_q) & L_{dq\_HF}(i_d,i_q)\\ L_{qd\_HF}(i_d,i_q) & L_{q\_HF}(i_d,i_q)\end{bmatrix}\frac{d}{dt}\begin{bmatrix}\Delta i_d\\ \Delta i_q\end{bmatrix} \quad (2)$$

where Δ represents the difference between the two neighboring switching periods, $L_{d\_HF}(i_d,i_q)$, $L_{q\_HF}(i_d,i_q)$ are the load-dependent dq-axes HF self-inductances respectively and $L_{dq\_HF}(i_d,i_q)$ is the load-dependent HF cross-coupling inductance caused by the cross-saturation effects due to the load current.

Since $L_{dq\_HF}(i_d,i_q)=L_{qd\_HF}(i_d,i_q)$ [16], (2) could be decoupled by transforming it into a special $d'q'$ reference frame, where the d'-axis leads the d-axis by an angle of ε (as illustrated in Fig. 2). This transformation gives (3), where $u_{d'}$, $u_{q'}$, $i_{d'}$, $i_{q'}$ are the stator voltages and currents respectively in the $d'q'$-reference frame. ε is the load-dependent position error caused by the cross-saturation effects. It can be found that ε should satisfy (4) for removing the cross-coupling term. In this sense, this d'-axis is regarded as the magnetic d-axis.

$$\varepsilon=\frac{1}{2}\cdot\arctan\frac{2L_{dq\_HF}(i_d,i_q)}{L_{d\_HF}(i_d,i_q)-L_{q\_HF}(i_d,i_q)} \quad (4)$$

When considering sensorless operation, since only estimated position information can be obtained, it is needed to transform (2) to the estimated $\hat{d}\hat{q}$-frame, and (5) can then be obtained

$$\begin{bmatrix}\Delta u_{\hat{d}}\\ \Delta u_{\hat{q}}\end{bmatrix}=\begin{bmatrix}L_0+L_1\cos 2(\tilde{\theta}_r+\varepsilon) & L_1\sin 2(\tilde{\theta}_r+\varepsilon)\\ L_1\sin 2(\tilde{\theta}_r+\varepsilon) & L_0-L_1\cos 2(\tilde{\theta}_r+\varepsilon)\end{bmatrix}\frac{d}{dt}\begin{bmatrix}\Delta i_{\hat{d}}\\ \Delta i_{\hat{q}}\end{bmatrix}$$
$$L_0=\frac{L_{d\_HF}(i_d,i_q)+L_{q\_HF}(i_d,i_q)}{2} \quad (5)$$
$$L_1=-\frac{\sqrt{[L_{d\_HF}(i_d,i_q)-L_{q\_HF}(i_d,i_q)]^2+4L_{dq\_HF}^2(i_d,i_q)}}{2}$$

where $u_{\hat{d}}$, $u_{\hat{q}}$, $i_{\hat{d}}$, $i_{\hat{q}}$ are the stator voltages and currents respectively in the estimated $\hat{d}\hat{q}$-reference frame; $\tilde{\theta}_r$ is the

$$\begin{bmatrix}\Delta u_{d'}\\ \Delta u_{q'}\end{bmatrix}=\begin{bmatrix}L_{d'\_HF}(i_d,i_q) & 0\\ 0 & L_{q'\_HF}(i_d,i_q)\end{bmatrix}\frac{d}{dt}\begin{bmatrix}\Delta i_{d'}\\ \Delta i_{q'}\end{bmatrix}$$
$$L_{d'\_HF}(i_d,i_q)=\frac{L_{d\_HF}(i_d,i_q)+L_{q\_HF}(i_d,i_q)}{2}-\frac{\sqrt{(L_{d\_HF}(i_d,i_q)-L_{q\_HF}(i_d,i_q))^2+4L_{dq\_HF}^2(i_d,i_q)}}{2} \quad (3)$$
$$L_{q'\_HF}(i_d,i_q)=\frac{L_{d\_HF}(i_d,i_q)+L_{q\_HF}(i_d,i_q)}{2}+\frac{\sqrt{(L_{d\_HF}(i_d,i_q)-L_{q\_HF}(i_d,i_q))^2+4L_{dq\_HF}^2(i_d,i_q)}}{2}$$

This article has been accepted for publication in a future issue of this journal, but has not been fully edited. Content may change prior to final publication. Citation information: DOI 10.1109/TIA.2019.2958792, IEEE Transactions on Industry Applications

position estimation error between the real rotor position (θ_r) and the estimated rotor position ($\hat{\theta}_r$), i.e. $\tilde{\theta}_r = \theta_r - \hat{\theta}_r$ as indicated in Fig. 3(a). When the injection scheme is chosen as Fig. 2(a), where two opposite voltage vectors are injected only on the estimated $\hat{d}$ -axis, the following equation can be obtained as:

$$\begin{bmatrix} 2U_{\hat{d}} \\ 0 \end{bmatrix} \approx \begin{bmatrix} L_0 + L_1\cos 2(\tilde{\theta}_r + \varepsilon) & L_1 \sin 2(\tilde{\theta}_r + \varepsilon) \\ L_1 \sin 2(\tilde{\theta}_r + \varepsilon) & L_0 - L_1 \cos 2(\tilde{\theta}_r + \varepsilon) \end{bmatrix} \frac{d}{dt} \begin{bmatrix} \Delta i_{\hat{d}} \\ \Delta i_{\hat{q}} \end{bmatrix} \quad (6)$$

Following a similar equation derivation process given in [19], it is found that the position information is contained in the estimated q-axis ($\hat{q}$) current as:

$$\frac{d\Delta i_{\hat{q}}}{dt} \approx \frac{\Delta(\Delta i_{\hat{q}})}{T_s} = \frac{-2L_1 U_{\hat{d}}}{L_0^2 - L_1^2} \sin(2\tilde{\theta}_r + 2\varepsilon) \quad (7)$$

where T_s is the switching period. It is obvious that from (7), only $\tilde{\theta}_r + \varepsilon = (\theta_r - \hat{\theta}_r) + \varepsilon = 0$ can be obtained from the measurable variable $\Delta(\Delta i_{\hat{q}})$ by feeding it to a PLL position estimator (Fig. 2(b)). Thus $\hat{\theta}_r = \theta_r + \varepsilon$, and the estimated $\hat{d}$ -axis aligns with the d′-axis, leading the real rotor position by an angle of ε, as shown in Fig. 3(b).

In order to estimate the real rotor d-axis, the position estimation error ε has to be obtained from other methods. Fig. 4 shows the measured average load-dependent position error ε at different loads with the assistance of an encoder and $\varepsilon = \hat{\theta}_r - \theta_r$. The red marks in Fig. 4 are the measured results and the dashed line is the fitted curve. It is obtained that ε is zero when i_q=0A, since there is no cross-coupling, i.e. $L_{dq\_HF}(i_d, i_q) = 0$. To achieve an ideal no-load condition, the load machine is controlled to provide a positive torque cancelling the frictional torque (therefore zero q-axis current). The measured average position error becomes zero, as shown in Fig. 4. Moreover, it clearly shows that ε increases when the load (q-axis current) increases. This linear behavior is not unique for this machine. Similar profiles can be found for other machines using different sensorless methods as well [1], [13], [17].

III. Proposed Method Based on Torque Equation

A. Load Dependennt Position Error Detection Based on the Torque Equation

As discussed in section II, based on the voltage equation, without the knowledge of the load-dependent HF inductances, the position estimation error ε cannot be determined or identified by the sensorless algorithm itself. However, for online identification, it might be possible to take the advantage of constant machine torque when running the machine at steady state. The torque equation, which is well-known as given in (8), can be used as a new method for the load-dependent position error ε online detection.

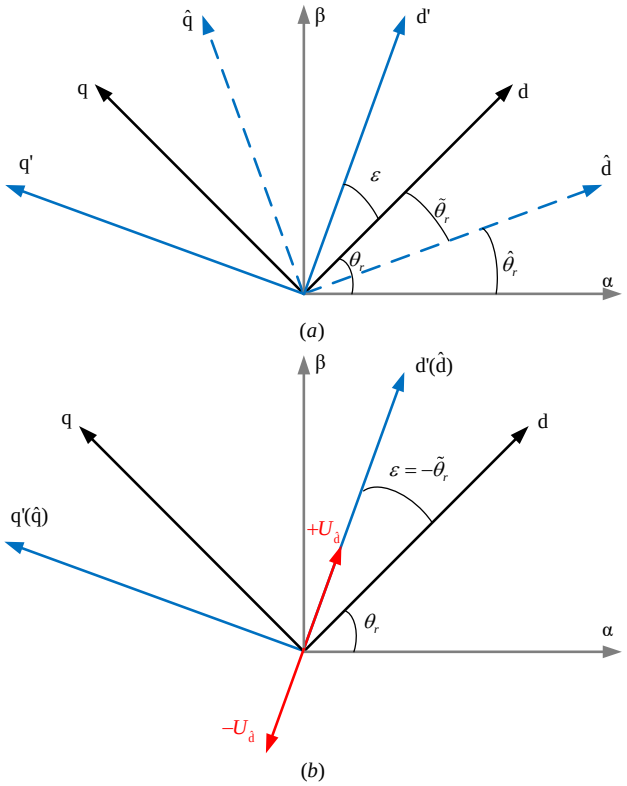

Fig. 3. (a) Relationship between different reference frames, d, d′ and $\hat{d}$ -axes representing the real (unsaturated), machine magnetic (saturated) and estimated rotor positions respectively; (b) under sensorless operation.

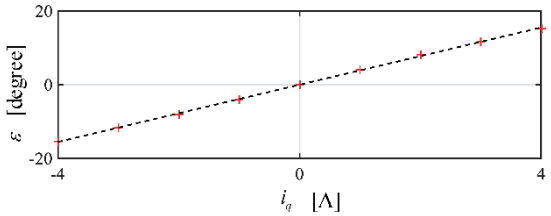

Fig. 4. Measurement result of the average load-dependent position error ε under different load conditions. Red marks are the measurement values and the dashed line is the fitted curve.

$$T_e = \frac{3}{2} p[\lambda_{mpm} i_q + (L_d - L_q) i_d i_q] \quad (8)$$

T_e is the electromagnetic torque and p is the number of pole pairs.

The torque equation given in (8) is related to the real dq-axes currents. However, in sensorless drives, only the estimated position and the current components on the estimated dq-axes are available. The load-dependent position error ε will

This article has been accepted for publication in a future issue of this journal, but has not been fully edited. Content may change prior to final publication. Citation information: DOI 10.1109/TIA.2019.2958792, IEEE Transactions on Industry Applications

introduce errors to the dq-currents used for the torque estimation, as:

$$T_{e0}=\frac{3}{2}p\lambda_{mpm}i_1\sin(\beta_1+\varepsilon_0)+\frac{3}{2}p(L_d-L_q)i_1\sin(\beta_1+\varepsilon_0)i_1\cos(\beta_1+\varepsilon_0) \quad (9)$$

where T_{e0} is the load torque; ε_0 is the load-dependent position error corresponding to this load torque T_{e0}; i_1 is the current vector magnitude of an operation point and β_1 locates this current vector with respect to the d′-axis, as illustrated in Fig. 5. It could be observed that there are two unknowns ε_0 and T_{e0} in (9). If the constant load torque T_{e0} could be obtained by a torque transducer, then for this particular torque, ε_0 could be solved based on (9). But to use a torque transducer in the drive system is not realistic. Therefore in order to solve for the two unknowns, one more equation based on (9) but at another operation point i_2 should be introduced. This is achieved by simply varying the current vector angle β from β_1 to β_2. Then the two unknowns could be obtained by solving the two equations based on i_1 and i_2 with the motor parameters listed in the experiment section Table II.

Equation (9) is a nonlinear equation and is difficult to get its solution. An intuitive way showing the principle of the proposed method is illustrated in Fig. 6. Angle ε is unknown, but we could allow this angle to change from -90 degrees to 90 degrees artificially, then the corresponding torque can be obtained from (9) for these two different operation points. The intersection point is the solution of these two equations, where $\varepsilon=\varepsilon_0$ and $T_e=T_{e0}$, as illustrated in Fig. 6.

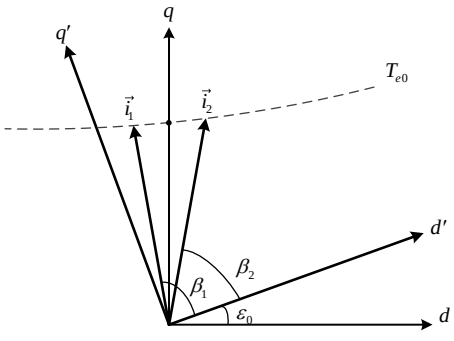

Fig. 5. Load-dependent position error ε_0 detection based on torque equation.

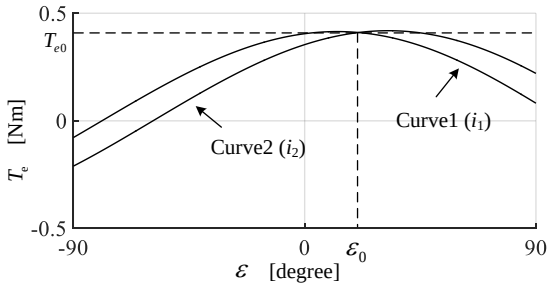

Fig. 6. Two curves of estimated torque versus estimated load denpedent position error based on the obtained operation points (i_1, i_2) for the same load torque (T_{e0}).

B. Simple Load-dependent Position Error Detection of SPMSM Neglecting the Saliency

Fig. 6 is only used to illustrate the basic idea of the proposed load-dependent position estimation error identification method. To solve the two nonlinear equations analytically for finding ε_0 is not easy. Easy-to-implement calculation methods that can be used online to find the intersection point ε_0 of the two T_e versus ε curves need to be developed. Since the reluctance torque is low in SPMSM, if neglecting the saliency of SPMSM, the torque equation (8) can then be simplified to

$$i_q=T_e\Big/(\frac{3}{2}p\lambda_{mpm}). \quad (10)$$

For the same load torque, the line linking the two terminals of two different current vectors ($\vec{i}_1$, $\vec{i}_2$) will be parallel to the real d-axis as shown in Fig. 7. Thus the real d-axis can be detected by simply varying the current vector angle. The implementation procedure is shown below.

First, the current vector is applied to the estimated q-axis, i.e. $i_{\hat{d}}=0$ and $\beta_1=90°$, and the actual current vector $\vec{i}_1$ required at this operation condition can be recorded. Then the current vector is rotated to a new position, where the angle is changed to β_2. The actual current vector $\vec{i}_2$ required for the same load torque can be obtained. Finally, the direction of $\vec{i}_2-\vec{i}_1$ (red vector in Fig. 7) can be obtained, which is aligned with the machine real d-axis, since the vector $\vec{i}_2-\vec{i}_1$ must be perpendicular to the machine real q-axis, for producing the same motor torque. The load-dependent position error can then be calculated in the estimated dq-axes, as:

$$\varepsilon_0=-\arctan\frac{i_{\hat{q}2}-i_{\hat{q}1}}{i_{\hat{d}2}-i_{\hat{d}1}}=-\arctan\frac{i_2\sin(\beta_2)-i_1\sin(\beta_1)}{i_2\cos(\beta_2)-i_1\cos(\beta_1)} \quad (11)$$

It is observed from (11) that no machine parameters are need in (11) for finding the desired load dependent position estimation error.

This article has been accepted for publication in a future issue of this journal, but has not been fully edited. Content may change prior to final publication. Citation information: DOI 10.1109/TIA.2019.2958792, IEEE Transactions on Industry Applications

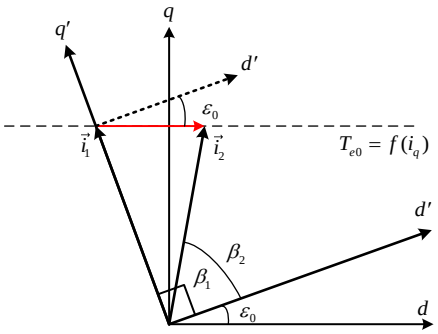

Fig. 7. Simple load-dependent position error ε_0 detection method.

C. *Load-dependent Position Error Detection and Compensation for SPMSM with Saliency*

In SPMSM the d-axis is often slight saturated by the permanent magnet, which introduces a small saliency. The above proposed simple ε detection method neglecting the saliency may be further extended to handle the SPMSM with machine saliency. It should be noted that the machine torque curve is no longer parallel to the machine d-axis, due to the existence of the machine reluctance torque. There is an angle shift δ between the real d-axis and the direction of $\vec{i}_2 - \vec{i}_1$, as shown in Fig. 8. The new constant torque (T_{e0}) curve could be drawn according to the following equation, which is derived from (8).

$$i_q = f(i_d) = \frac{2T_{e0}}{3p[\lambda_{mpm} + (L_d - L_q)i_d]} \tag{12}$$

According to Lagrange's mean value theorem, there exists a point $i_{d0} \in (i_{d1}, i_{d2})$ that makes $\left.\frac{di_q}{di_d}\right|_{i_{d0}} = \frac{i_{q2} - i_{q1}}{i_{d2} - i_{d1}}$. This means the slope of the line formed by $\vec{i}_2 - \vec{i}_1$ (therefore the angle δ) in the real machine dq-axes can be calculated by:

$$\begin{aligned} &\frac{i_{q2} - i_{q1}}{i_{d2} - i_{d1}} = \left.\frac{di_q}{di_d}\right|_{i_{d0}} = \frac{2T_{e0}}{3p} * \frac{-(L_d - L_q)}{[\lambda_{mpm} + (L_d - L_q)i_{d0}]^2} \\ &\delta = \arctan\frac{i_{q2} - i_{q1}}{i_{d2} - i_{d1}} \end{aligned} \tag{13}$$

Comparing Fig. 8 with Fig. 7, it can be noted that the vector $\vec{i}_2 - \vec{i}_1$ is no longer aligned with the machine real d-axis, but with an error of δ. Moreover, it should be noticed that the current used in (13) is in the real dq-reference frame, which is different from the current components used in (11). Besides, the current i_{d0} is unknown. However, for SPMSM with saliency, due to the fact that the PM torque is predominant and the reluctance torque is small, i_d is much smaller than i_q, and $(L_d - L_q)i_{d0} \ll \lambda_{mpm}$. Then the error δ can be estimated as:

$$\delta \approx \arctan[\frac{2T_{e0}}{3p} * \frac{-(L_d - L_q)}{(\lambda_{mpm})^2}] \tag{14}$$

Since the reluctance torque is small, similar to (10), the machine torque needed in (14) can be estimated by:

$$T_{e0} \approx \frac{3}{2} p\lambda_{mpm} i_{\hat{q}1} \tag{15}$$

Therefore, the angle caused by the involvement of the reluctance torque can be estimated by:

$$\delta \approx \arctan\frac{(L_q - L_d)i_{\hat{q}1}}{\lambda_{mpm}} \tag{16}$$

The $\hat{\varepsilon}$ to be estimated includes two components accordingly (due to the PM interaction torque (11) and due to the reluctance torque (16), respectively):

$$\begin{aligned} \varepsilon_0 = &-\arctan\frac{i_2\sin(\beta_2) - i_1\sin(\beta_1)}{i_2\cos(\beta_2) - i_1\cos(\beta_1)} \\ &+ \arctan\frac{(L_q - L_d)i_1\sin(\beta_1)}{\lambda_{mpm}} \end{aligned} \tag{17}$$

It can be observed from (17) that no HF inductances or cross-saturation inductances (as indicated in (7)) are required in the calculation of ε_0. Only the constant fundamental frequency inductances L_d, L_q and PM flux λ_{mpm}, which can be obtained by machine parameter identification methods e.g. [21] or from motor datasheet, are involved in the calculation. For example, in this paper, the constant fundamental frequency inductances L_d and L_q are measured by a simple current step response of a RL equivalent circuit of the machine at no load and zero speed. λ_{mpm} is obtained from the machine speed constant given in the datasheet.

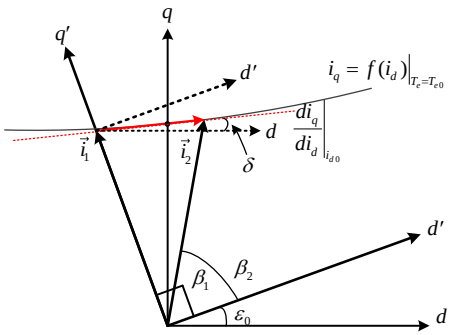

Fig. 8. Load-dependent position error ε_0 detection considering the reluctance torque.

When L_d and L_q are not equal, the additional angular shift δ of the vector linking the terminals of the current vectors at

This article has been accepted for publication in a future issue of this journal, but has not been fully edited. Content may change prior to final publication. Citation information: DOI 10.1109/TIA.2019.2958792, IEEE Transactions on Industry Applications

two different locations will appear as shown in Fig. 8 and (13), which is further simplified to (16). When deriving (16), it is assumed that the torque is calculated by the q-axis current in the estimated frame, i.e. (15). This estimated frame q-axis current may differ from the real q-axis current due to the existence of the position estimation error ε_0 (Fig. 8). The influence of neglecting ε_0 in (15) and (16) is discussed below using the parameters of the PMSM listed in Table II:

When the machine is operated with an encoder and under full load toque ($i_q = 4\mathrm{A}$), the position error ε_0 is changed manually from -20 degrees to 20 degrees. It is clear from Fig. 8 that β_1 for locating current vector $\vec{i}_1$ is 90 degrees away from the estimated d-axis, i.e. $\left|\vec{i}_1\right| = i_{\hat{q}1}$. The angle δ could be calculated from (16) for different ε_0 values as:

TABLE I. ε_0 INFLUENCE ON (16)

ε_0 [degree]	-20	-10	0	10	20
δ [degree]	6.4	6	5.8	5.8	6

When $\varepsilon_0 = 0°$, $\vec{i}_1$ is on the real q-axis and the estimated frame q-axis current is the real q-axis current. It is at the ideal situation. When $\varepsilon_0 = -20°$, $i_{\hat{q}1}$ used in (16) is at its worst case in this study. But it could be observed from Table I that when $\varepsilon_0 = -20°$, the calculated $\delta = 6.4°$, where there is less than one degrees error compared to the ideal situation value of $\delta\big|_{\varepsilon_0=0°} = 5.8°$. In addition, it should be pointed out that (16) is the second term of the calculated position error of (17). The first term in (17) is not affected by this angle δ . Thus, this less than one degrees error introduced by using (16) to approximate (13) or (14) will have even less influence in (17).

The load-dependent position error ε detected by the proposed method, can be compensated when performing pulse-based sensorless control to the drive system, as illustrated in Fig. 9.

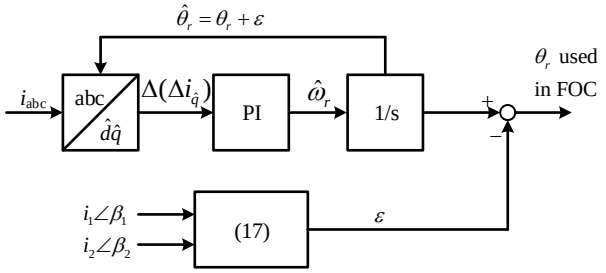

Fig. 9. Position estimation error compensation.

The flow chart of the proposed load-dependent position estimation error compensation method is summarized in Fig. 10. First, during the steady state operation with the pulse-based sensorless method (7), the current i_1 can be obtained while $\beta = \beta_1$. Then the current angle is changed to β_2 to obtain $\vec{i}_2$. Thereafter, according to (17) the load-dependent position error can be calculated and compensated consequently as shown in Fig. 9. It should be pointed out that this detection method should be applied each time when a load torque variation is detected.

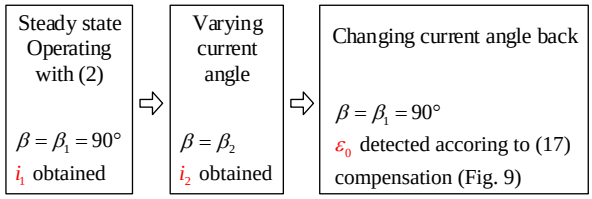

Fig. 10. Flow chart of the proposed load-dependent position error compensation method.

IV. EXPERIMENTAL VERIFICATION AND DISCUSSIONS

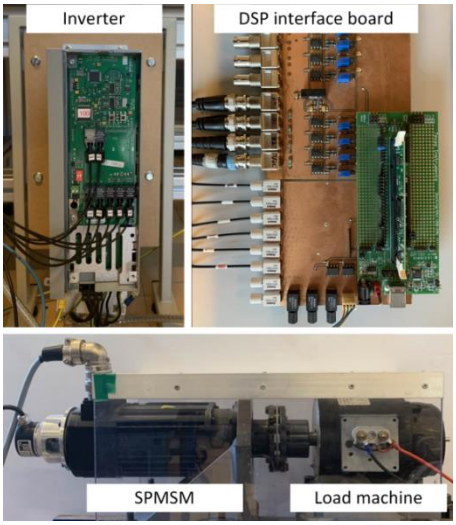

Fig. 11. Experimental setup for testing the proposed method.

TABLE II. PARAMETERS OF THE USED SPMSM

Parameters of SPMSM	
Rated power [W]	400
Max. phase voltage [V]	380
Rated current (RMS) [A]	2.9
Rated speed [rpm]	2850
Rated frequency [Hz]	95
Stator resistance [Ω]	2.3
d-axis inductance L_d [mH]	10
q-axis inductance L_q [mH]	13
PM flux linkage [Wb]	0.12
Pole pairs	2
System inertia [kg·m^2]	1e-3

This article has been accepted for publication in a future issue of this journal, but has not been fully edited. Content may change prior to final publication. Citation information: DOI 10.1109/TIA.2019.2958792, IEEE Transactions on Industry Applications

A SPMSM drive system, as shown in Fig. 11, is built to verify the proposed load-dependent position estimation error detection method. The parameters of the SPMSM are listed in Table II. A 500W DC motor is employed as the load machine. A Danfoss FC302 voltage source inverter is used to drive the SPMSM, where the control is achieved through a DSP-TMS320F28335 with a switching frequency of 5 kHz. An incremental encoder with 2048 lines per revolution is mounted on the SPMSM to provide the reference of the real rotor position.

To show the phenomenon of the position estimation error caused by the load current in low speed sensorless drive, an experiment is carried out with 50% load step at 15 rpm as shown in Fig. 12. It can be seen from Fig. 12 that before load step the average position error is -1.2°, which is due to the small no-load current for overcoming the frictional torque. After 50% load step, the position estimation error $\tilde{\theta}_r$ reaches -8.4°, which is mainly due to the cross-saturation effects caused by the load current.

According to the aforementioned load-dependent position error detection method described in section III.A, two different working points are chosen as current vectors located at $\beta_1 = 90°$ (for normal operation) and at $\beta_2 = 78°$ (for detection), respectively. Regarding the value of β_2, first it is preferred to choose $\beta_2 < \beta_1$ to keep the operation point not further away from the desired operation point, since the load dependent position error is $\varepsilon > 0$ in PMSM. If $\beta_1 - \beta_2$ is too small, then the difference between i_1 and i_2 may be too small to be regarded as two different working points. In the experiment, it is observed that when $\beta_1 - \beta_2$ is larger than 10 degrees, the two operation points show a clear difference.

In Fig. 12, at about 10s, the second current vector angle at $\beta_2 = 78°$ is applied for 2s (with obvious estimated d-axis current appearing). Then two steady state operation points can be obtained. With these two points, the two estimated torque curves can be formed (as Fig. 6) with the intersection point identified to be at $\varepsilon_0 = 8°$ (as shown in Fig. 13), which agrees well with the measured value of 8.4° from the encoder. However, observing the intersection point from the two curves shown in Fig. 13 (as the ideal solution) is difficult to be implemented online.

For online calculation, according to section III.C, with these two measurement points, the estimated load-dependent position error can be calculated directly from (17), which gives a good estimation of $\varepsilon_0 = 7.6°$. After the 2s implementation of the current vector angle β_2, the current vector angle varies back to $\beta_1 = 90°$ with the identified ε_0 of 7.6° compensated, as shown in Fig. 12. It could be observed that the position estimation error $\tilde{\theta}_r$ is only -0.8° after compensation, which shows the effectiveness of the proposed load-dependent position estimation error online detection method.

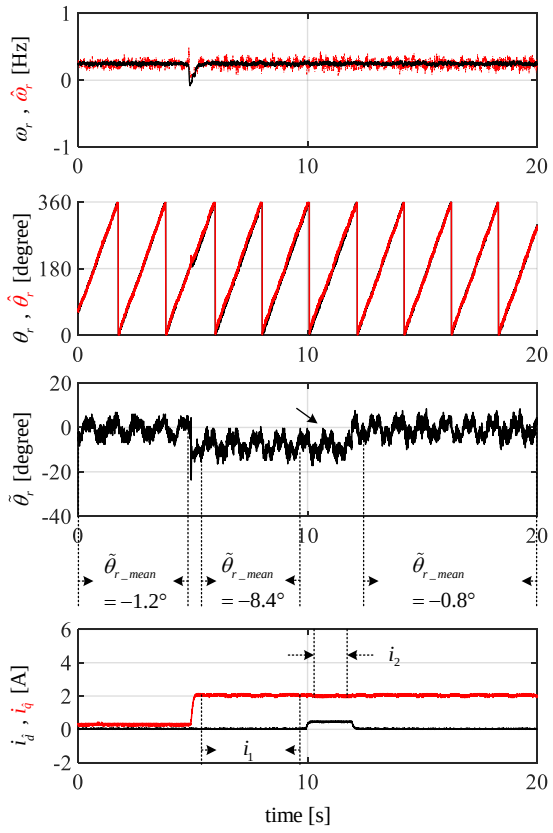

Fig. 12. Experimental results of the position sensorless drive under 50% load torque step at 15 rpm with position error compensation. From top to bottom: real and estimated speed, real and estimated rotor position, position error, machine currents in the estimated dq-frame.

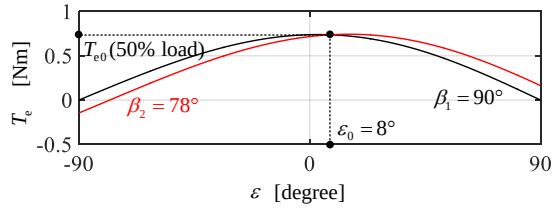

Fig. 13. Two curves of estimated torque versus position estimation error based on the experimentally obtained operation points (i_1, i_2) with 50% load torque.

This article has been accepted for publication in a future issue of this journal, but has not been fully edited. Content may change prior to final publication. Citation information: DOI 10.1109/TIA.2019.2958792, IEEE Transactions on Industry Applications

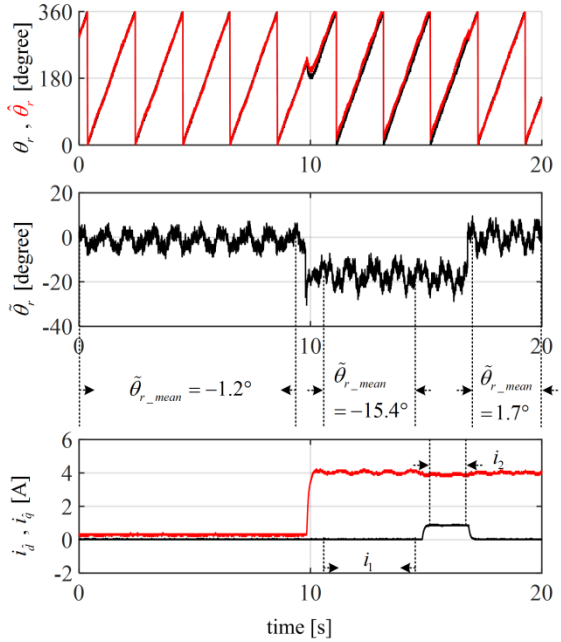

Fig. 14. Experimental results of the position sensorless drive under 100% load torque step at 15 rpm with position error compensation. From top to bottom: real and estimated rotor position, position error, machine currents in the estimated dq-frame.

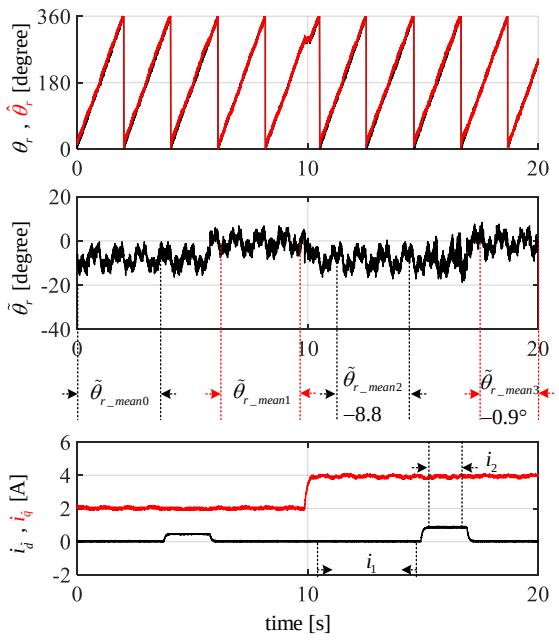

Fig. 15. Experimental results of the position sensorless drive with load torque step from 50% to 100% at 15 rpm with position error compensation. From top to bottom: real and estimated rotor position, position error (where $\tilde{\theta}_{r\_mean0} = -8.4°$, $\tilde{\theta}_{r\_mean1} = -0.8°$, $\tilde{\theta}_{r\_mean2} = -8.8°$, $\tilde{\theta}_{r\_mean3} = -0.9°$), machine currents in the estimated dq-frame.

Fig. 14 shows the performance of the SPMSM drive using the proposed method with 100% load step at 15 rpm. It could be seen that a big position estimation error $\tilde{\theta}_r = -15.4°$ is present with 100% load. With the proposed method two working points can be obtained with the current vector placed at 90 and 78 degrees respectively, and the estimated load-dependent position error from (17) is $\varepsilon_0 = 17.1°$. After compensation, the average position estimation error $\tilde{\theta}_r$ becomes 1.7° only.

It should be noted that the proposed method should only be performed at steady state. Therefore, when the load change is detected by the speed feedback, the proposed method should be performed after the system reaches a new steady state again as shown in Fig. 15. First a 50% load is applied to the sensorless system similar to Fig. 12, where the position estimation error $\tilde{\theta}_r$ is -0.8° with the compensation angle of $\varepsilon_0 = 7.6°$. Thereafter a full load torque step, the proposed method is applied again giving a new result $\varepsilon_0 = 8.3°$. Thus after compensation the average position estimation error $\tilde{\theta}_r$ becomes -0.9°.

Since the proposed method (17) is parameter dependent, the parameter sensitivity is therefore analyzed below. Assuming the parameter $(L_d - L_q)$ will change ±30% comparing with the real machine parameter, the obtained load-dependent position errors by following the same principle shown in Fig. 6, are shown in Fig. 16. It could be observed from Fig. 16 that in case of ±30% parameter inaccuracy, there will be less than 2 degrees error in the proposed detection method. Correspondingly, the calculated position estimation errors using the simplified implementation approach, i.e. (17), are $\varepsilon|_{70\%(L_d - L_q)} = 15.5°$, $\varepsilon|_{100\%(L_d - L_q)} = 17.1°$, $\varepsilon|_{130\%(L_d - L_q)} = 18.9°$ respectively, agreeing well with the results indicated in Fig. 16. Meanwhile, during normal operation, the real PM flux may decrease together with the decrease of ($L_d - L_q$) due to the saturation effects, which means the values used in the calculation based on (17) will be higher than the real saturated machine parameters. Therefore, 120% λ_{mpm} and 130% $(L_d - L_q)$ are applied in (17). The calculated position estimation error in this case is $\varepsilon|_{130\%(L_d - L_q)\ \&\ 120\%\lambda_{mpm}} = 17.7°$, which shows a better result than the calculation result with 130% $(L_d - L_q)$ change only.

Although the previous study based on dedicated Finite Element Analysis and other studies such as [9], [28] have proven that the distorted inductance profiles caused by load current related saturation will introduce position estimation error, other issues like the sensorless method itself may also

This article has been accepted for publication in a future issue of this journal, but has not been fully edited. Content may change prior to final publication. Citation information: DOI 10.1109/TIA.2019.2958792, IEEE Transactions on Industry Applications

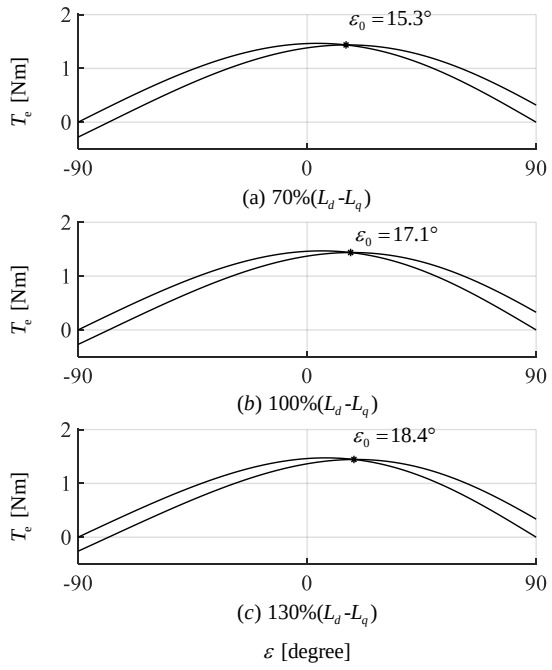

Fig. 16 Parameter sensitivity verification, position estimation error calculation based on inaccurate parameters (a) 70%($L_d - L_q$); (b) 100% $(L_d - L_q)$; (c) 130%($L_d - L_q$).

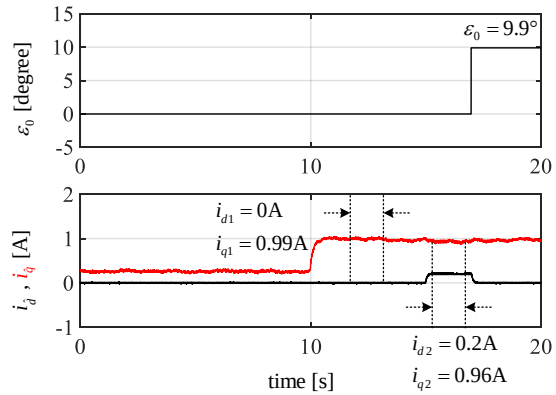

Fig. 17 Experimental results with 10 degrees pre-set position error.

introduce position estimation error. It is worth to point out here that the proposed method in principle is an universal position error detection and compensation method. Not only the error introduced by the cross-saturaiton efftects but also the error from other sources could be detected by the proposed method. To verify this, an experiment is carried out where an articicial error of 10 degrees is added to the rotor real position. The detection method used in other experiments is used here (i.e. $\beta_1 = 90°$ and $\beta_2 = 78°$) and the estimated-frame $\hat{d}\hat{q}$ currents are shown in Fig. 17. The calculation result by using the measured currents and (17) is 9.9 degrees, which matches the pre-set error very well.

The proposed method is based on the torque equation. As long as accurate machine parameters are used, it can give accurate results. However, in this paper, a great effort is made to allow to use machine datasheet parameters for simplified calculation and online implementation, instead of solving two nonlinear equations (e.g. (9) and Fig. 6).

Besides its possible online application feature, the proposed method may also be considered as a calibration method for saliency tracking based sensorless methods for SPMSM. The sensorless drive needs to be connected to a load and is in speed control mode, which is quite common for a normal test bench. Without the needs of an extra shaft-locking device, dedicated hardware for accurate PWM voltage measurement or accurate inverter nonlinear voltage error compensation for flux map measurement, the position error could be detected and then compensated by simply varying the orientation of the current vector.

V. Conclusion

In this paper, the position estimation error caused by the load current in HF injection sensorless drive is analyzed first. Then a simple and effective method to online detect and compensate the load-dependent position estimation error is proposed especially for SPMSM sensorless drive in low speed range, without requiring additional devices or HF inductances information. In speed controlled mode and in steady state, the proposed method beneficially utilizes the torque equation which is much less influenced by the cross-saturation effects that often introduce difficult-to-compensate position estimation errors when using the machine voltage equations and HF signal injection methods for position estimation in the low speed range. It has been demonstrated that the proposed method can effectively detect the load-dependent position estimation error by simply varying the orientation of the current vector. Satisfactory results are obtained when the load-dependent position error compensated.

References

[1] J. Holtz, "Developments in Sensorless AC Drive Technology," *International Conference on Power Electronics and Drives Systems*, vol. 1, pp. 9-16, 2005.

[2] I. Boldea, M. C. Paicu, and G. D. Andreescu, "Active Flux Concept for Motion-Sensorless Unified AC Drives," *IEEE Transactions on Power Electronics.*, vol. 23, no. 5, pp. 2612-2618, 2008.

[3] M. W. Degner, R. D. Lorenz, "Using Multiple Saliencies for the Estimation of Flux, Position, and Velocity in AC Machines," *IEEE Transaction on Industry Applications*, vol. 34, no. 5, pp. 1097-1104, 1998.

[4] J. H. Jang, S. K. Sul, J. I. Ha, K. Ide, M. Sawamura, "Sensorless Drive of Surface-Mounted Permanent-Magnet Motor by High-Frequency Signal Injection Based on Magnetic Saliency," *IEEE Transaction on Industry Applications*, vol. 39, no. 4, pp. 1031-1038, 2003.

[5] Y. Young-Doo, S. Seung-Ki, S. Morimoto, and K. Ide, "Highbandwidth sensorless algorithm for ac machines based on square-wave-type voltage injection," *IEEE Transaction on Industry Applications*, vol. 47, no. 3, pp. 1361-1370, 2011.

[6] M. Schroedl, "Sensorless Control of AC Machines at Low Speed and Standstill Based on the "INFORM" Method," *31st IAS Annual Meeting, Conference Record of the 1996 IEEE*, vol. 1, pp. 270-277, 1996.

[7] H. Wang, K. Lu, D. Wang and F. Blaabjerg. "Identification of load current influences on position estimation errors for sensorless SPMSM drives," *Proc. APEC,* pp 533-539, 2018.

[8] Y. Inoue, K. Yamada, S. Morimoto, M. Sanada, "Effectiveness of Voltage Error Compensation and Parameter Identification for Model-Based Sensorless Control of IPMSM," *IEEE Transactions on Industry Applications*, vol. 45, no. 1, pp. 213-221, 2009.

[9] Z. Q. Zhu, Y. Li, D. Howe, C. M. Bingham. "Compensation for Rotor Position Estimation Error due to Cross-Coupling Magnetic Saturation in Signal Injection Based Sensorless Control of PM Brushless AC Motors," *Proc. IEMDC*, pp.208-213, 2007.

[10] S. Ebersberger, B. Piepenbreier "Identification of Differential Inductances of Permancet Magnet Synchronous Machines Using Test Current Signal Injection," *Proc. Symp. Power Electronics, Electrical Drives, Automation and Motion*, pp. 1342-1347, 2012.

[11] P. Landsmann, R. Kennel "Q-axis pulse based identification of the anisotropy displacement over load for surface mounted PMSM". *Proc. SLED/PRECEDE*, pp. 1–6, 2013.

[12] N. Teske, G. M. Asher, M. Sumner. K.J Bradley. "Suppression of saturation saliency effects for the sensorless position control of induction motor drives under loaded conditions," *IEEE Transactions on Industry electronics*. vol. 47, no. 5, pp. 1142-1150, 2000.

[13] P. Landsmann, D. Paulus, and R. Kennel, "Online identification of load angle compensation for anisotropy based sensorless control," *Proc. SLED*, vol. 2, pp. 80-84, 2011.

[14] K. Wiedmann and A. Mertens, "Self-sensing control of pm synchronous machines including online system identification based on a novel mras approach," *Proc. SLED*, vol. 3, pp. 21-22, 2012.

[15] H. Wang, K. Lu, D. Wang and F. Blaabjerg. "Investigation of Various Position Estimation Accuracy Issues in Pulse-Injection-based Sensorless Drives," to be published on ECCE-ASIA 2018.

[16] D. Mingardi, M. Morandin, S. Bolognani, N. Bianchi, "On the Proprieties of the Differential Cross-Saturation Inductance in Synchronous Machines", *IEEE Trans. on Ind. Appl.,* vol. 53, no. 2, pp. 991 - 1000, 2017.

[17] J. M. Liu, Z. Q. Zhu. "Novel Sensorless Control Strategy with Injection of High-Frequency Pulsating Carrier Signal into Stationary Reference Frame," *IEEE Trans. Ind Appl*. vol. 50, no. 4, pp. 2574-2583, 2014.

[18] P. Guglielmi, M. Pastorelli, A. Vagati. "Cross saturation effects in IPM motors and related impact on zero-speed sensorless control," *Proc. of IEEE Fourtieth IAS Annual Meeting Conference on Industry Applications*, pp. 2546-2552, 2005.

[19] H. Wang, K. Lu, D. Wang and F. Blaabjerg. "Simple and Effective Position Estimation Error Compensation Method for Sensorless SPMSM Drives," *Proc. ECCE*, pp. 1710-1715, 2018.

[20] Z.Q. Zhu, L.M. Gong. "Investigation of Effectiveness of Sensorless Operation in Carrier-Signal-Injection-Based Sensorless-Control Methods," *IEEE Trans. on Ind Electron*. vol. 58, pp. 3431-3439, no. 8, 2011.

[21] S. A. Odhano, P. Giangrande, R. I. Bojoi, C. Gerada. "Self-Commissioning of Interior Permanent- Magnet Synchronous Motor Drives With High-Frequency Current Injection," *IEEE Trans. Ind Appl*. vol. 50, no. 5, pp. 3295-3303, 2014.

[22] D. Xu, B. Wang, G. Zhang, G. Wang, Y. Yu. "A review of sensorless control methods for AC motor drives," *CES Transactions on Electrical Machines and Systems*. vol. 2, no. 1, pp. 104 - 115, 2018.

[23] M. Hinkkanen, P. Pescetto, E. Molsa, S. E. Saarakkala, G. Pellegrino, and R. Bojoi, "Sensorless self-commissioning of synchronous reluctance motors at standstill without rotor locking," IEEE Trans. Ind. Appl., vol. 53, no. 3, pp. 2120–2129, May/Jun. 2017.

[24] Q. Wang, G. Zhang, G. Wang, C. Li and D. Xu "Offline Parameter Self-Learning Method for General-Purpose PMSM Drives With Estimation Error Compensation," *IEEE Transactions on Power Electronics.*, vol. 34, no. 11, pp. 11103-11115, 2019.

[25] L. Peretti, P. Sandulescu, and G. Zanuso, "Self-commissioning of flux linkage curves of synchronous reluctance machines in quasi-standstill condition," IET Elect. Power Appl., vol. 9, no. 9, pp. 642–651, 2015.

[26] N. Bedetti, S. Calligaro, and R. Petrella, "Stand-still self-identification of flux characteristics for synchronous reluctance machines using novel saturation approximating function and multiple linear regression," IEEE Trans. Ind. Appl., vol. 52, no. 4, pp. 3083–3092, Jul./Aug. 2016.

[27] Z. Q. Zhu, Y. Li, D. Howe, C. M. Bingham, and D. Stone, "Influence of machine topology and cross-coupling magnetic saturation on rotor position estimation accuracy in extended back-EMF based sensorless PM brushless AC drives," In Proc. 42nd IAS Annu. Meet.,2007, pp. 2378-2385

[28] R. Ni, D. Xu, F. Blaabjerg, K. Lu, G. Wang, and G. Zhang, "Square-wave voltage injection algorithm for PMSM position sensorless control with high robustness to voltage errors," IEEE Trans. Power Electron., vol. 32, no. 7, pp. 5425–5437, Jul. 2017.